International Journal of Fluid Power 13 (2012) No. 2 pp. 15-28

COUPLED SIMULATION OF A TELEHANDLER FORKS HANDLING HYDRAULICS

G. Altare, F. Lovuolo, N. Nervegna and M. Rundo

Fluid Power Research Laboratory
Politecnico di Torino, Corso Duca degli Abruzzi 24, 10129 Torino, Italia
gabriele.altare@polito.it, francesco.lovuolo@polito.it, nicola.nervegna@polito.it, massimo.rundo@polito.it

Abstract

The paper presents the development of the simulation model of the forks handling system of a telehandler. The study has been performed through coupled simulation of two software codes, AMESim for the 1D modelling of hydraulics and Virtual Lab for the mechanical modelling of the telescopic boom and forks. In context the advantage is that coupled simulation involves just one integrator with significant savings in computer time. Aim of the analysis is the development of a validated model capable of predicting system behaviour with adequate accuracy in different operating conditions. Following a kinematic analysis to evidence the characteristics of the mechanical system, such as the automatic forks levelling, forks lever ratio and overrunning load conditions, the detailed hydraulics modelling is discussed with emphasis on overcentre valves. The hydraulic model is interfaced with the mechanical one that based on forces consequent to load induced pressures evaluates in turn velocities and displacements. The complete model received experimental validation through significant boom and forks duty cycles. A fair agreement has been reached confronting experimental and predicted outcomes.

Keywords: coupled Simulation, overcentre valves, telehandler.

1 Introduction

Earthmoving and off-road vehicles manufacturers manifest a growing interest in coupling kinematics/dynamics of the boom and implements with the hydraulics devised to perform required duties. Reasons to investigate this topic are twofold: in the first place to account for actuators loads dependence on boom and forks position and in the second place to optimize boom/forks layout geometry to increase manoeuvre speed while keeping force amplification on actuators at a minimum. The vehicle where this mechanical-hydraulic coupling has been investigated is a commercial telehandler. These units are in wide use in agriculture as well as in industrial and civilian environments due to their versatile performance. In fact they behave as wheel loaders when fitted with a bucket, as forklifts when the bucket is replaced by forks and as cranes if winches are employed. In all these applications, as the boom is lifted, the load transferred to the actuator is not constant. The same occurs when either the forks or the bucket are tilted. The opening or closing of the bucket/forks and the lifting/lowering of the boom form the object of attentive analyses by hydraulic designers being these manoeuvres the most recurrent. It is therefore clear that due account should be given to the kinematics/dynamics of the boom/forks characteristics when devising dedicated hydraulics to drive this system.

Different software codes are available that allow analysis of mechanic-hydraulic systems coupling. Some handle both aspects while others are specifically oriented either to one or to the other domain. In the first category fall AMESim with its Planar Mechanical library (Altare, 2009) and Matlab/Simulink with SimMechanics (Prabhu, 2007). The second approach requires use of appropriate interfaces to exchange variables from one to the other domain during simulation. One example involves Co-Simulation between AMESim and ADAMS (Roccatello, Mancò and Nervegna, 2007) or between AMESim and Virtual Lab Motion (Prescott, 2009). However, the continuous transfer of information heavily impacts simulation time. More recently another possibility is being granted by Coupled Simulation (Prescott, 2009). This essentially avoids use of two separate integrators for the state equations and, consequently, warrants faster simulations. This is the case when AMESim - Virtual Lab Motion are used in synergy in a coupled simulation environment.

This manuscript was received on 22 September 2011 and was accepted after revision for publication on 18 January 2012

This paper investigates this novel approach applied to the boom and forks handling hydraulics of a Merlo telehandler shown in Fig. 1.

Fig. 1: *View of the telehandler vehicle(Italian patent number 0001378243 (30 July 2010))*

2 Telescopic boom

2.1 System description

Figure 2 shows the system under study. This is comprehensive of a two element telescopic boom that bears, through mechanical links and leverages, the forks implement. Two dedicated double acting linear actuators, namely the telescopic boom (TBA) and forks cylinder (FA), respectively allow variation of boom inclination up to about 70 degrees and forks swing within about 140 degrees with reference to a horizontal plane. The third movement involves a third actuator (housed inside the boom) that allows the boom extension. Both single and simultaneous commands on boom and forks can be effected. In addition an automatic hydraulic forks levelling system exists through an additional linear actuator (FLA). Accordingly, as boom is lifted or lowered, forks are kept parallel to the ground without operator's intervention.

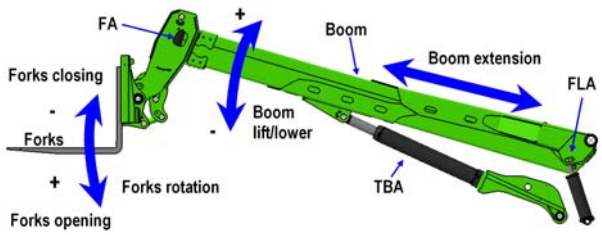

Fig. 2: *Movements of telescopic boom and forks*

2.2 Hydraulic Circuit

Figure 3 shows the hydraulic circuit supplying the three linear actuators cited above. The boom actuator TBA is fed by a closed centre load sensing proportional directional control valve (PDCV1), while forks rotation is controlled by a float centre similar valve PDCV2. Both directional valves feature post-compensation to prevent loss of controllability in case of flow saturation. If the boom is lifted or lowered, an automatic forks levelling is enacted, since actuator FLA maintains an initially set position for the forks implement (usually parallel to ground). In fact, as the boom is lifted, the FLA rod, hinged at the boom, undergoes an extension.

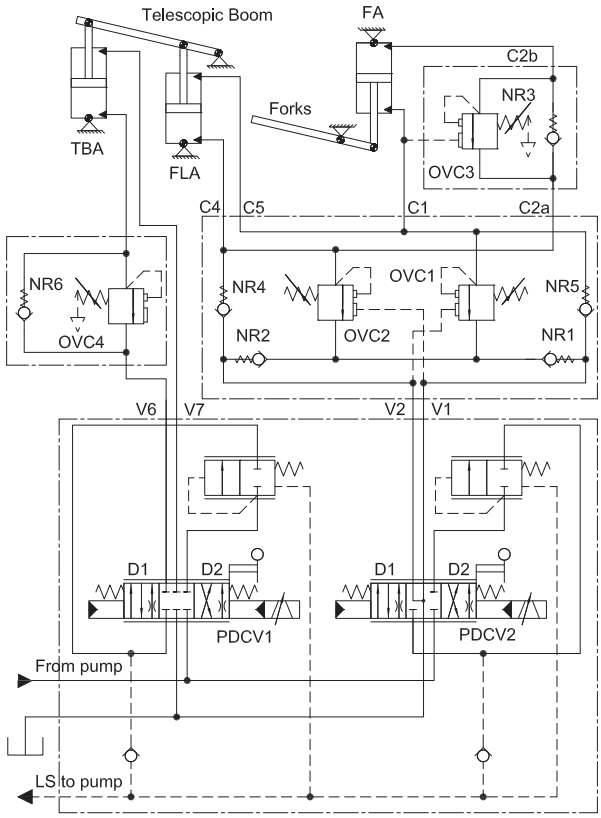

Fig. 3: *The hydraulic circuit*

A volume of fluid is then transferred from the rod side chamber of FLA to the rod side chamber of FA. For this to happen, overcentre valves OVC1 and OVC2 remain shut while valve OVC3 allows the discharge of fluid from the FA bore chamber. This fluid fills the increasing volume of the FLA bore chamber. Fluid volumes transfer between the two actuators must also rely on their dimensioning to properly attain an automatic forks levelling as boom position is changed. During the lowering of the boom, the overcentre valve OVC4 generates a back pressure in the bore chamber of the actuator TBA in order to control overrunning loads. If the boom stays fixed and the working position D1 of the proportional valve PDCV2 is active, then the system tends to close the forks (negative rotation due to FA extension). In fact the working fluid, bypassing OVC2 and OVC3 through check valves NR4 and NR3, feeds the bore chamber of FA. The return line collects fluid discharged from the FA rod side under control of OVC1. Thereafter the fluid, crossing NR1, goes back to tank through the PDCV2. Conversely, if PDCV2 is actuated in the position D2 the forks are opened (positive rotation due to FA retraction). The flow generation unit, not represented in Fig. 3, is made up of a variable displacement load sensing pump with differential and absolute

pressure limiters. Within the flow generation unit a bleed orifice connects the global load sensing pilot line to tank when all directional valves are in their neutral position. The unit also feeds other hydraulic systems such as the hydrostatic power steering and the actuator in charge of the extension/retraction of the boom. Table 1 collects attainable effects upon intervention on PDCV1 and PDCV2.

Table 1: Obtainable effects actuating PDCV1 and PDCV2

PDCV1 D1	Boom lift (positive rotation) Automatic forks levelling (FA retraction)
PDCV1 D2	Boom lower (negative rotation) Automatic forks levelling (FA extension)
PDCV2 D1	Forks negative rotation (Closing – FA extension)
PDCV2 D2	Forks positive rotation (Opening - FA retraction)

2.3 Kinematics

The analysis of system kinematics has considered three aspects: (1) the evaluation of the Forks Lever Ratio (*FLR*) binding the load force acting on the forks (GK" = 600 mm) with force F_P that the forks actuator (*FA*) has to withstand; (2) the development of an analytic relation to express force F_{TBA} required to lift the boom when subjected to F_{LOAD} and its own weight; (3) the assessment of the automatic forks levelling system to appraise the angular mismatch with respect to an horizontal reference plane.

The forks lever ratio FLR is not constant; in fact, as the *FA* stroke (*FAs*) varies, linkages are such that force F_{LOAD}, is transferred onto the FA actuator rod as a variable quantity both in module and direction.

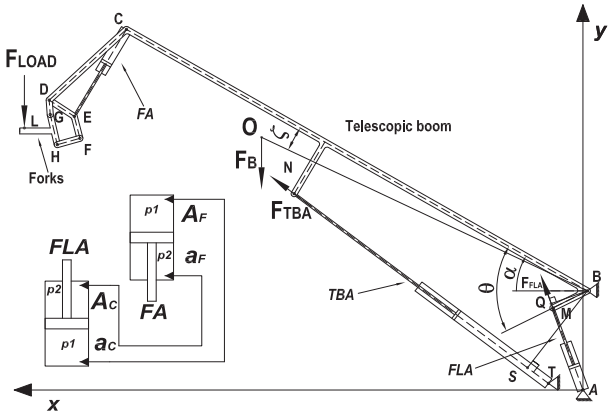

Fig. 4: *Boom and forks kinematics*

With reference to Fig. 4 and Fig. 5, forks rotational equilibrium about hinge *G* leads to Eq. (1):

$$F_{\text{Load}}\ \overline{GK'}(FAs) = F_{\text{H}}\,\overline{GR}(FAs) \tag{1}$$

While, about hinge *D*, the equilibrium of element with vertices *D*, *E* and *F* evaluates to Eq. (2):

$$F_H\,\overline{DZ}(FAs) = F_{\text{p}}\ \overline{DU}(FAs) \tag{2}$$

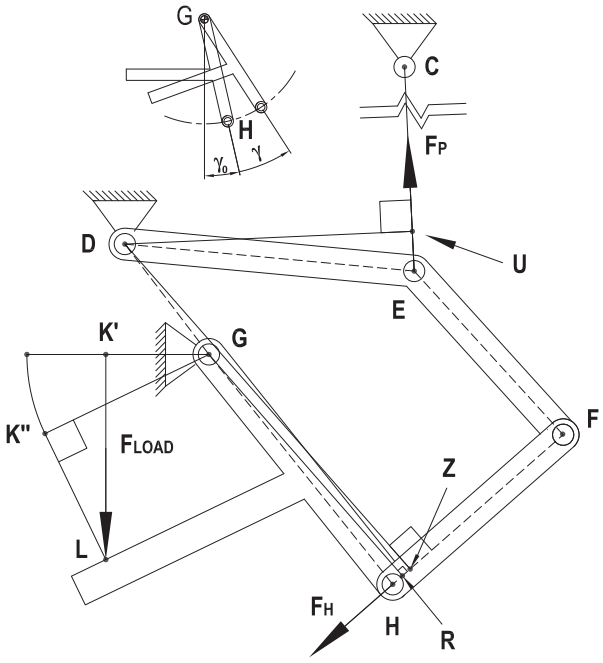

Fig. 5: *Zoom of the forks handling system*

This further leads to Eq. (3) that describes the behaviour of *FLR* as function of the *FAs*:

$$FLR(FAs) = \frac{F_{\text{p}}(FAs)}{F_{\text{Load}}} = \frac{\overline{DZ}(FAs)\ \overline{\text{GK}'}(\text{FAs})}{\overline{GR}(FAs)\ \overline{DU}(FAs)} \tag{3}$$

Depending on operating conditions, the line of action of force F_{LOAD} changes with respect to the forks. In fact, a condition is considered where, being load perpendicular to ground, forks are rotated keeping boom tilt constant. The situation is depicted in Fig. 6 where it can be argued that, as the *FAs* changes, the same load behaves as either resistant or overrunning (due to the change of sign between the external load F_{LOAD} and the force on the forks actuator).

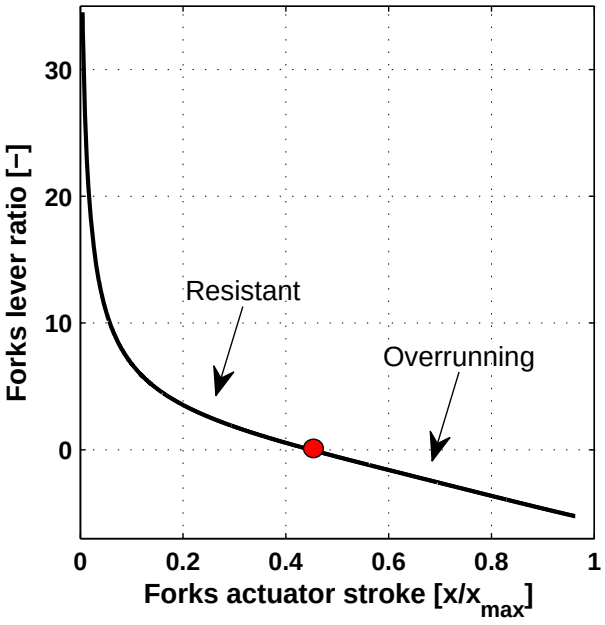

Fig. 6: *Forks lever ratio vs. forks actuator stroke*

During retraction from a fully extended state load is overrunning up to a limit of 45 % of the full stroke. It then turns resistant with a considerable increase in the forks lever ratio and load amplification. In the extension phase the situation is obviously reversed.

A quite frequent mode of operation involves the lift/lower of the boom with forks parallel to ground and charged by a load. In this specific condition where the load is perpendicular to the forks and ground, the actuator stroke *FAs* depends on angle α due to the automatic forks levelling system. Consequently, *FLR* can be expressed as function of boom tilt only as shown in Fig. 7 where it can be observed to vary between 4.6 and 5.1. These are relatively low values if compared with those attained previously (see Fig. 6).

Equation (3) links F_{LOAD} with F_{P}. Due to the hydraulic coupling (see top left of Fig. 4) actuator *FLA* exerts a force F_{FLA} on the boom that depends on F_{LOAD}. Since area ratios of both linear actuators are identical it is possible, considering Eq. (3), to express the relation between force F_{FLA} on the boom at hinge Q and force F_{LOAD} as follows:

$$F_{\mathrm{FLA}}(\alpha) = F_{\mathrm{Load}} \frac{\overline{DZ}(\alpha)\ \overline{\mathrm{GK}'}(\alpha)}{\overline{GR}(\alpha)\ \overline{DU}(\alpha)}\left(2-\frac{A_{\mathrm{C}}}{A_{\mathrm{F}}}\right) \tag{4}$$

Moreover, considering boom geometry and linkages it is possible, for a given load induced force $F_{LOAD,}$ to derive the relation yielding boom actuator force F_{TBA} as a function of boom inclination α. This dependence is expressed in Eq. (5) where due account is also taken of boom weight applied at its centre of mass O:

$$F_{\mathrm{TBA}}(\alpha) = \frac{\overline{OB}\cos(\alpha\text{-}\zeta)}{\overline{BS}(\alpha)}F_B + \frac{F_{\mathrm{LOAD}}}{\overline{BS}(\alpha)}\left[x_L(\alpha) - \overline{QB}(\alpha)\,FLR(\alpha)\left(2-\frac{A_{\mathrm{C}}}{A_{\mathrm{F}}}\right)\right] \tag{5}$$

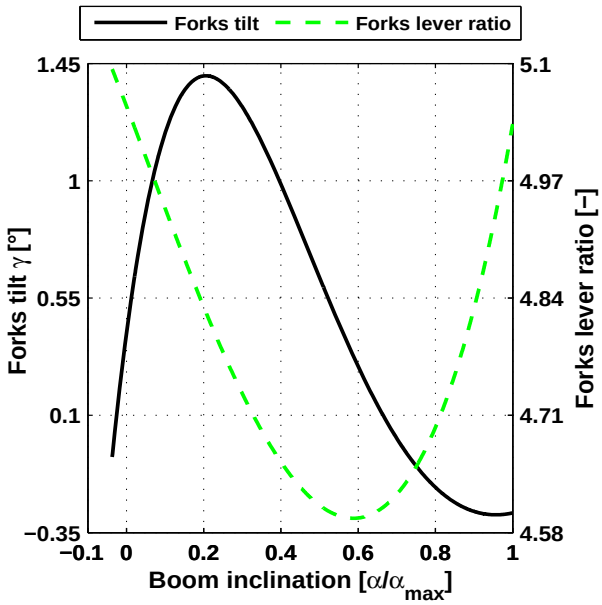

Fig. 7: *Forks inclination and lever ratio*

Fig. 8 reports force F_{TBA} vs. boom inclination for three different load conditions on the forks and precisely null ($F_{\mathrm{L},1}$), intermediate ($F_{\mathrm{L},2}$) and maximum load ($F_{\mathrm{L},3}$). The decreasing trend observed in all three traces is ascribable to the negative contribution of F_{FLA} that reduces F_{TBA} as α is increased. In addition, the dependence of F_{FLA} on F_{LOAD} is responsible for the evident F_{TBA} slope increase as F_{LOAD} is also increased.

A further characteristic quantity analysed is the levelling error γ. With reference to Fig. 4, the evaluation of γ requires knowledge of the positions of revolute joints *G* and *H* and of the stroke of actuators FA and FLA as functions of angle α. Through Eq. (7) it is possible to express the position of point M as function of α and, sequentially evaluate the FLA stroke:

$$\begin{cases} x_{\mathrm{M}}(\alpha) = x_{\mathrm{B}} + \overline{BM}\cos(\theta-\alpha) \\ y_{\mathrm{M}}(\alpha) = y_{\mathrm{B}} + \overline{BM}\sin(\theta-\alpha) \end{cases} \tag{3}$$

Moreover, the hydraulic coupling between the FA and FLA actuators leads to Eq. (7):

$$\left(\overline{MA}(\alpha) - l_{\mathrm{cc}}\right)\alpha_{\mathrm{c}} = \left(\overline{CE}(\alpha) - l_{\mathrm{fc}}\right)\alpha_{\mathrm{f}} \tag{4}$$

from which distance $\overline{CE}(\alpha)$ can be appraised.

Trigonometric relationships applied to the polygon DEFHG, allow to determine coordinates of points *G* and *H*. Finally the dependence of angle γ as function of α is expressed by Eq. (8):

$$\gamma(\alpha) = \operatorname{atan}\left(\frac{x_{\mathrm{G}}(\alpha) - x_{\mathrm{H}}(\alpha)}{y_{\mathrm{G}}(\alpha) - y_{\mathrm{H}}(\alpha)}\right) - \gamma_0 \tag{8}$$

Figure 7 reports the behaviour of the forks levelling error as boom inclination is changed. It can be noticed that the maximum tilt reaches only 1.4° over the complete travel of the boom actuator. In this respect it should be observed that actuators have been so sized to attain minimum levelling mismatch.

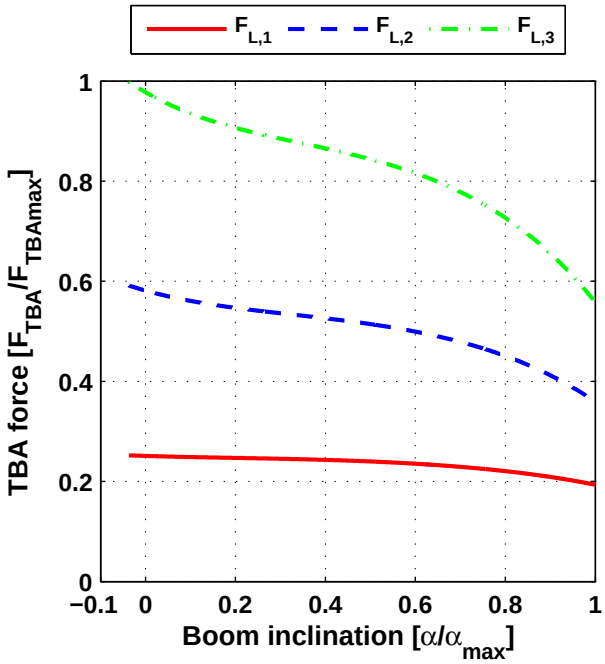

Fig. 8: *Force F_{TBA} vs. α for three values of F_{LOAD}*

3 Overcentre Valves

3.1 Single Valve OVC3

Figure 9 shows a section view of valve OVC3 with port designations, while in Fig. 10 the pertinent ISO scheme is reported.

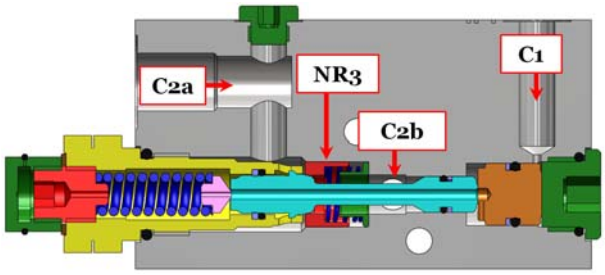

Fig. 9: *Section view of OVC3 valve*

The valve features a double cone poppet with sharp edge seat and an actuator with surface of influence S_3 on which the pilot pressure acts. The rod, integral with the poppet, is held in contact against the actuator by a spring with equivalent pressure setting p_3*. At rest, the seat is kept in contact against the poppet by a spring with pressure setting pNR_3*. The free flow from port C_{2a} to port C_{2b} is allowed by the movement of the seat to the right (non-return valve NR_3). Conversely, the oil can flow from C_{2b} to C_{2a} due to the movement to the left of the poppet under the action of the actuator thrust and the force induced by upstream pressure acting on surface s_3.

The passage area opens thanks to the sleeve protrusions that prevent the seat to move to the left. Significant data of the valve are collected in Table 2. The valve is of the vented to ambient type. In fact, the OVC spring chamber as well as the left end portion of the rod are eventually exposed to ambient through a radial hole in the closing cap.

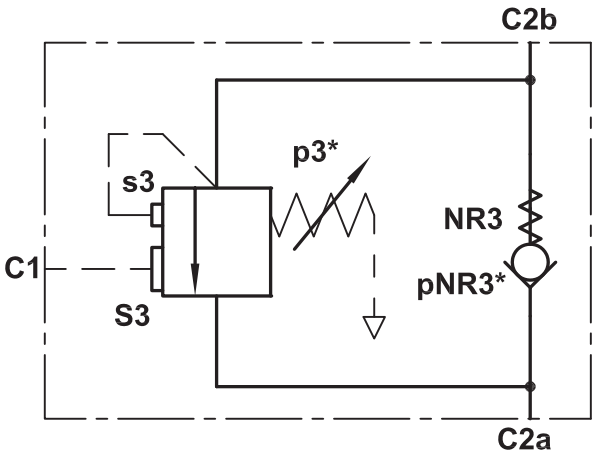

Fig. 10: *ISO scheme of OVC3 valve*

Table 2: Single overcentre valve data

Description	Value	Unit
Max pressure (p_{max})	350	bar
Max flow rate (Q_{max})	150	l/min

The valve has been simulated in the LMS Imagine.Lab AMESim environment starting from the geometrical quantities gathered by its 3D representation. The simulation model reported in Fig. 11 has been developed using the Hydraulic Component Design library. The variable passage area is simulated by two cone shaped poppets connected in parallel with different overlaps. Fixed restrictors and volumes take into account the pressure drop and the capacitance effects of the internal passageways.

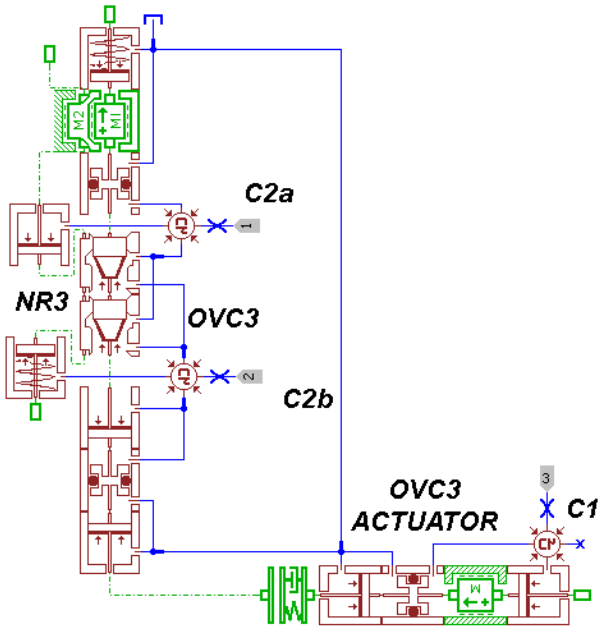

Fig. 11: *Detailed model of OVC3 valve*

The O-ring friction is considered by a suitable model available in the seal data library. The model also accounts for the steady-state contribution of the flow force stemming from the axial component of the momentum change.

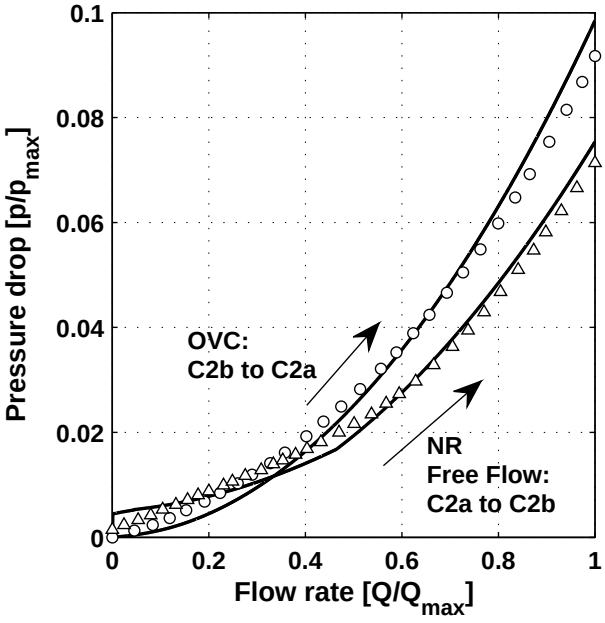

Fig. 12: *Comparison between simulated and experimental pressure drop at maximum opening (For Q_{max} and p_{max} values refer to Table 2)*

The valve model has been validated by comparing the simulated pressure drop (continuous line) as function of the flow rate with the corresponding characteristics published by the manufacturer (Fig. 12).

It can be noticed that the valve generates different pressure drops depending on the flow direction. This is due to the different maximum stroke of the actuator and the seat.

3.2 Dual Valve OVC1 and OVC2

The two overcentre valves OVC1 and OVC2 are integral within a single component featuring six ports. Figure 13 shows two orthogonal section views evidencing the two stages. Four ball check valves are also present. In Fig. 14 the ISO scheme of the complete assembly is reported. Each stage is made up of a poppet with a conical seat and an actuator with surfaces of influence S1 and S2. Unlike valve OVC3, the poppet seats are fitted with no clearance in the casing and the free flow is allowed by the ball poppet non-return valves. Two channels drilled in the poppet connect the spring chamber with the rod side volume of the actuator acting as dynamic (stabilizing) orifices.

Figure 15 shows the AMESim circuit of the OVC2 stage; the model of the OVC1 stage is symmetric except for the position of some internal junctions. The flow area generated by the poppet with respect to the conical seat is supplied with a data file evaluated from the 3D model.

The dual OVC valve model has been validated in the same manner as the single OVC valve (Fig. 16). The pressure drop (continuous lines for simulated curves) reported in the graph does not take into account the cracking pressure of non-return valves NR1 and NR2.

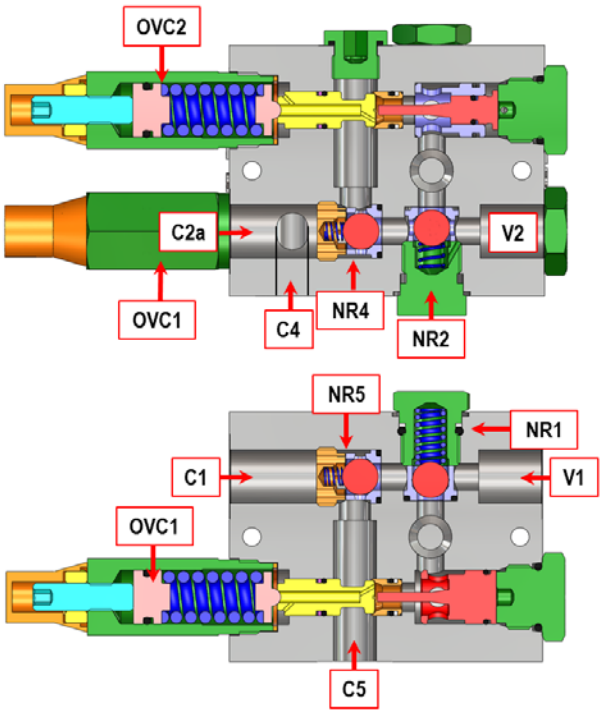

Fig. 13: *Section views of OVC2 and OVC1*

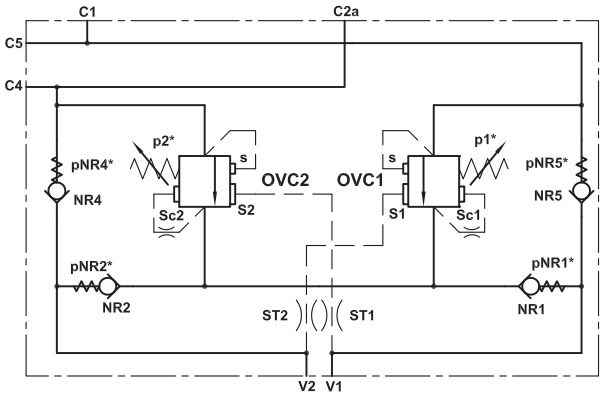

Fig. 14: *ISO scheme of dual OVC valve*

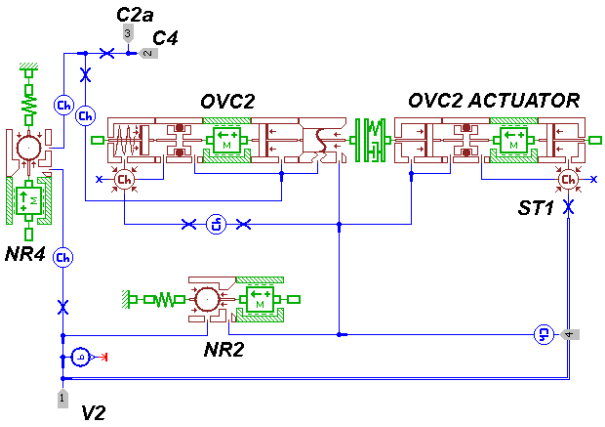

Fig. 15: *Detailed model of the dual OVC valve*

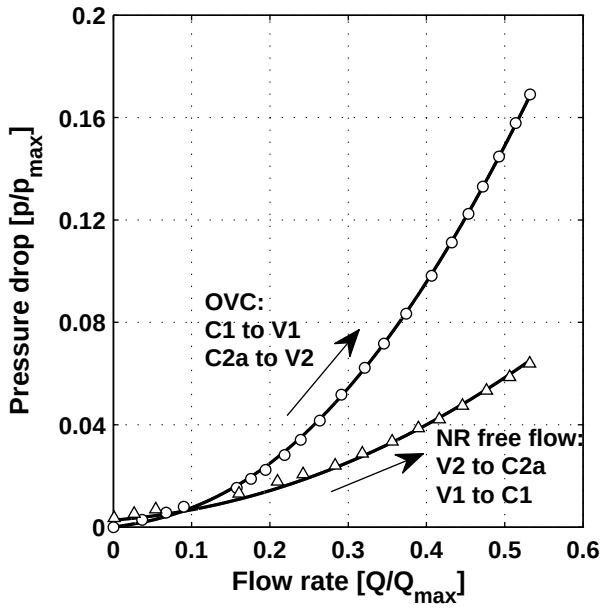

Fig. 16: *Comparison between simulated and experimental pressure drop at maximum opening (For Q_{max} and p_{max} values refer to Table 2)*

4 Simulation Approach

The entire system model has been developed in the LMS Imagine.Lab AMESim environment for the 1D modelling of the hydraulic circuit and in Virtual.Lab Motion (VLM) for the 3D mechanical modelling of the tele-

scopic boom and forks. Communication between the two codes evolves through an interface that allows importing the AMESim model into VLM. The opposite is also a feasible practice this basically resting on the decision of which solver will take the burden of advancing the solution of the system of constitutive equations. The choice relative to the solver was proved to be not influential on the solution and on stability. In effect while AMESim uses the DASSL (Differential Algebraic System Solver) solver, VLM makes use of BDF (Backward Differentiation Formula) that is one of 5 methods proper to DASSL. Consequently both environments use variable step/variable order methods. In the present study VLM was selected to solve system equations and in both codes all settings regarding tolerance, maximum step size, and error type have been left at their defaults. AMESim evaluates forces while VLM, through sensors, analyses bodies' dynamics in terms of position and velocity. These are then passed back to AMESim. System motion can then be tracked within VLM and animations related to all simulations analysed to gain further insight.

4.1 AMESim Model

Figure 19 shows the complete AMESim sketch of the system under study based on the ISO schematic reported earlier in the paper (Fig. 3).

In order to supply a realistic flow rate in terms of steady state and transient values, a variable displacement load sensing pump model has been developed (Fig. 17). The differential and absolute pressure limiters (DPL and APL respectively) have been designed with the Hydraulic Component Design Library, while the swash plate by the Mechanical Library. The volumetric pump efficiency at maximum displacement has been tuned on experimental curves published by the manufacturer (Bosch-Rexroth A10VO Technical data sheet, RE 92 703/10.07) at 1500 rpm and 2700 rpm.

Since tests were performed with the engine running at 2400 rpm available efficiency data have been interpolated. Figure 18 shows experimental and simulated pump volumetric efficiency vs. pump delivery pressure at 2400 rpm.

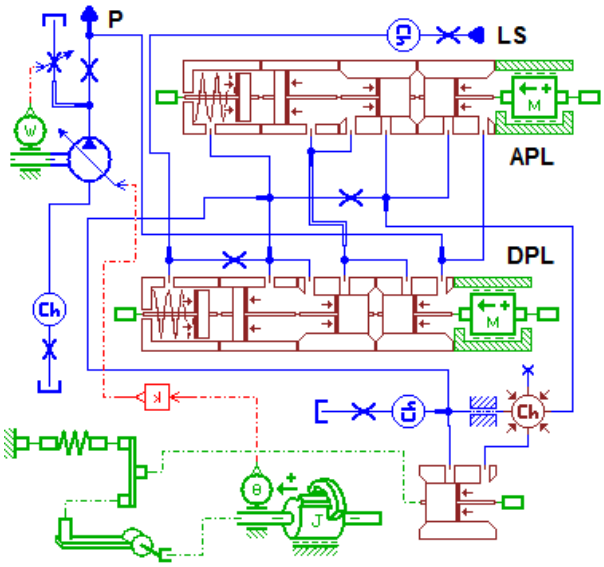

Fig. 17: *AMESim pump model*

Local and distributed pressure drops through hydraulic couplings and pipes have been assessed using components belonging to the Hydraulic Resistance library (AMESim User manual, 2010). However, to reduce the set of equations in the complete system, multiple hydraulic resistances in series have been lumped together and represented by equivalent restrictors. Suitable models were selected for hoses to account for their wall compliance characteristics.

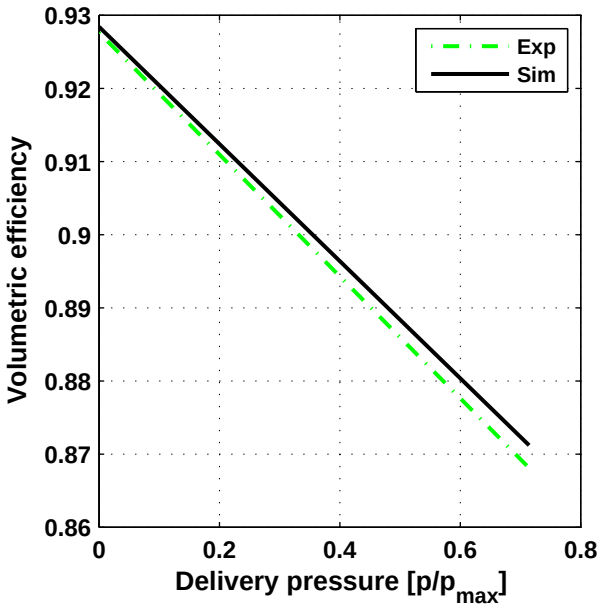

Fig. 18: *Experimental vs. simulated pump volumetric efficiency at maximum pump displacement*

Load sensing directional control valves modelled with the Hydraulic Library, have been tuned on characteristics published by the manufacturer. The same occurred for the boom overcentre valve. Other OVC valves in the system that were analysed in previous sections of the paper were then synthesized as "Supercomponents". The working fluid is an ISO VG 46 with a pressure dependent bulk modulus (12000 bar @ 20 bar; 18000 bar @ 210 bar). The system is considered in isothermal conditions at a fluid temperature of 50°C. Fig. 19 also shows the AMESim - VLM interface linked to the three linear actuators *TBA*, *FA* and *FLA*. As is often the case the telehandler besides the absolute pressure limiter is also equipped with a safety pressure relief valve. However this valve is never on duty during the experimental tests. Accordingly, it has been deliberately omitted from the AMESim model. The AMESim standard cylinder model allows users to set values for the coefficient of viscous friction due to fluid shear in the clearance spaces that result from the relative speed of the moving component. In lack of experimental data this speed dependent friction was set at 190 kN/(m/s) for the TBA and at 70 kN/(m/s) for the FA. Though high, these values also lump other contributions originated in system linkages (e.g. hinges). Their assessment was tuned at best on available data. The leakage coefficient has been set at 0.00035 (L/min)/bar based on experimental pressure decay in actuators chambers under static conditions.

4.2 Virtual Lab Motion Model

Analyses on the forks lever ratio (*FLR*) and telescopic boom force reported in the foregoing, bring to evidence that, due to existing linkages and centre of mass coordinates modification, extracting and retracting forces on linear actuators change as these travel along their work stroke. Consequently, fluid pressures undergo a continuous change. To properly account for this situation a multibody code VLM was selected and interfaced with the 1D simulation environment AMESim.

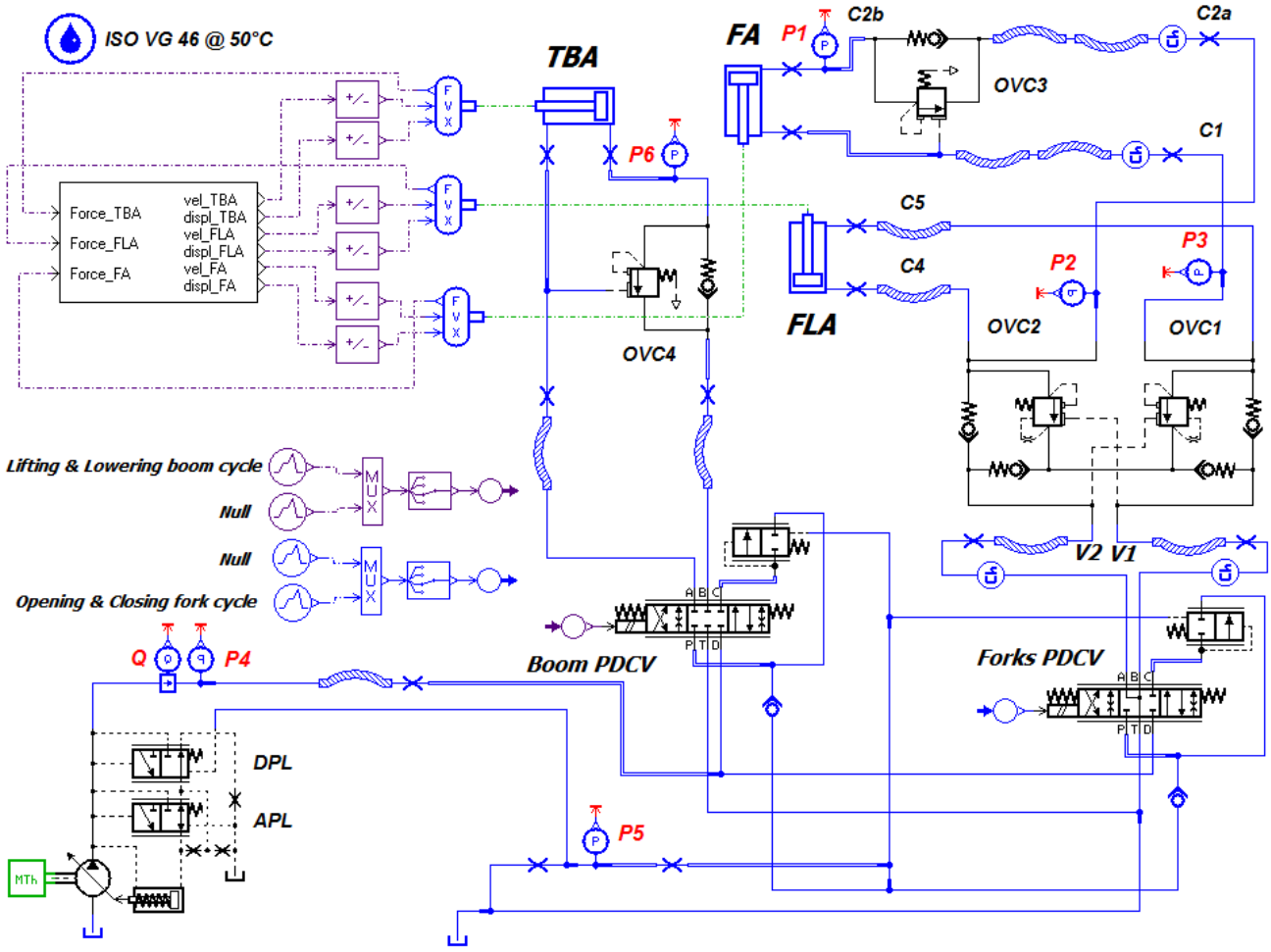

Fig. 19: *AMESIM simulation model layout*

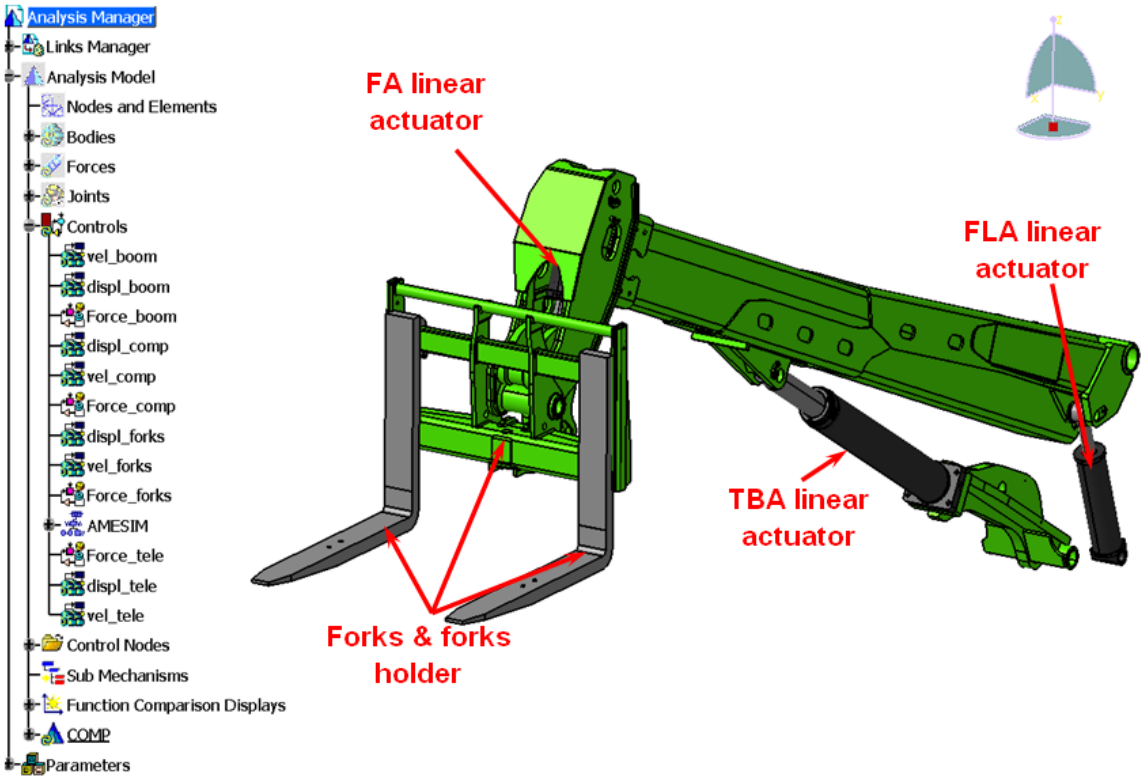

Fig. 20: *Virtual Lab Motion telescopic boom model*

VLM is based on the CATIA V5 graphics engine and features all required capabilities for a realistic multibody simulation, including modelling, solving and analysis. VLM offers an extensive list of joints and constraints and a library for force elements including stiffness, friction and end-stops. Thanks to the AMESim interface it allows linking of a 3D mechanism model with its 1D counterpart granting advantages of both software codes.

The connection is useful when studying the interaction between complex mechanism models and their hydraulic systems. This allows users to investigate dynamic performance and predict component and system loads through coupled simulation where state equations are solved as a complete set by the VLM simulation solver. Moreover the parametric approach leads to mechanical and hydraulic system optimization with feasible savings in prototyping development. A general overview of the approach is addressed in (Prescott, 2009). Import of the 3D model was effected through the Parasolid interface. The VLM model (Fig. 20) was further developed by assembling and linking all subassemblies to arrive at a complete virtual description of the boom and forks implement of the telehandler. Care was exercised in the definition of local coordinates reference systems for proper identification of mutual control variables. It is important to underline that the end-stop modelling is done within VLM by means of point-to-point contact elements. Loads acting on the forks are applied within VLM.

5 Model validation

5.1 Experimental Tests

Tests were conducted on a telehandler at the manufacturer's premises and allowed to acquire pressures and flow rates at various locations in the system. The diesel engine speed (directly driving the pump) and fluid temperature were also monitored and recorded. Figure 21 shows the sensors installation layout. Their basic characteristics are as follows:

- P1÷P6 pressure transducers Hydrotechnik, with measuring range 0 bar - 400 bar and accuracy ± 0.25 % F.S.
- Q flow meter Hydrotechnik, with measuring range 15 l/min - 307 l/min and error ±2.5 % F.S.

The engine was run at maximum speed and joysticks that drive the proportional directional control valves were instantly positioned either at their maximum tilt or left back to their rest so to replicate the various tests with identical and repeatable inputs. This was done purposely so to exercise possibly congruent input commands in the simulation model. Tests were specifically and uniquely oriented to the investigation of that portion of the hydraulic circuit that forms the object of the present studies.

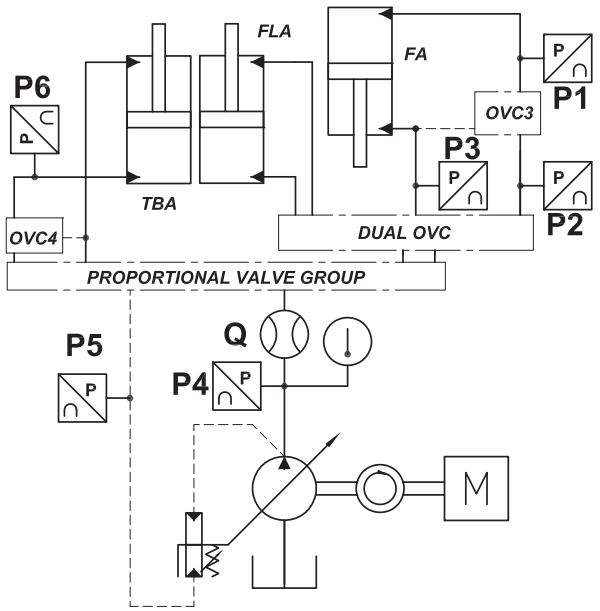

Fig. 21: *Sensors location*

Working manoeuvres considered during the test campaigns are as follows:

- lifting and lowering boom cycle (forks set parallel to ground).
- opening and closing forks cycle (boom at fixed position).

The working cycles are shown in Fig. 22 and are presented as dimensionless commands issued on the proportional valves vs. time. Though input commands are ideal square signals, the ensuing spools displacements are consequent to a second order dynamics that AMESim employs in standard directional valves modelling.

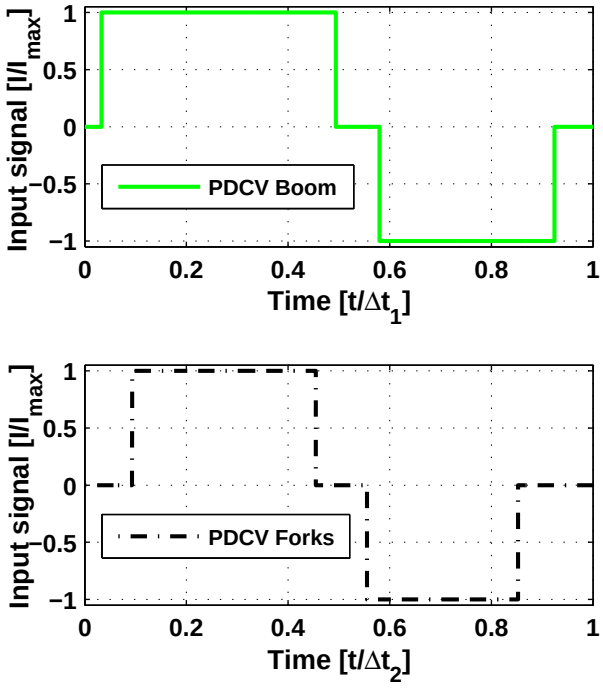

Fig. 22: *Boom and forks PDCV commands (Dt1=26s, Dt2=19s)*

5.2 Boom Lifting and Lowering Cycle

This work cycle consists in lifting and lowering the telescopic boom with forks parallel to ground. Starting with the boom at rest in a horizontal position and after a short initial delay a command is issued through the joystick onto the PDCV1 aiming at lifting the boom to its maximum inclination. The pump feeds the bore chamber of the TBA and the command is exercised beyond the time required to enact a complete extension of the actuator's rod. During swivel about hinge B the boom drags the FLA rod conveying oil into the rod end side of the FA actuator and thus promoting the return stroke of its rod. In turn, traversing the OVC3 valve, oil flows from the cap end side of FA into the cap end side of FLA. The automatic forks levelling process is then completed. Thereafter, the joystick is allowed to return to its rest position. Then it becomes fully shifted in the opposite direction to promote boom lowering until complete rod retraction is attained. As the boom is lowered oil volumes are exchanged between the FLA and FA actuators in the opposite fashion. In order that the hydraulic coupling be effective, piping links between the two linear actuators must remain isolated from the rest of the hydraulic circuit. This is in fact warranted by a fully closed dual OVC valve that hinders the connection of the proportional directional control valve PDCV2 with both actuators. Fig. 24 and Fig. 25 collect pressure signals at three locations in the system (P4, P5 and P6) along with pump flow rate and allow direct comparisons of measured (dashed lines) against simulated traces (continuous lines). In greater detail Fig. 24 shows pump delivery pressure (top) and load sensing pressure (bottom) as functions of time. Fig. 25 shows instead pressure at the bore chamber of the boom actuator (top) and the pump flow rate (bottom).

In the initial idling condition pump delivery pressure is held at about 0.07 p_{max} by the Differential Pressure Limiter (DPL). As the boom is lifted the pump operates at full displacement delivering a flow rate of 0.9 Q_{max} with a correspondent linear speed of the boom actuator of 0.11 m/s. A gradual lessening of all pressure signals, during boom lifting, can be observed that is consequent to the boom force variation addressed earlier in the paper. In this portion of the work cycle the difference between delivery and load sensing pressures is fairly constant at 0.07 p_{max}. The simulation model is in full agreement with experimental data. At about 0.4 Δt_1 seconds the rod of the TBA completes its outward travel and the pump absolute pressure limiter (APL) intervention off-strokes the pump restraining delivery pressure.

Due to the limited information on the load sensing pump and particularly on the dynamics of its displacement controls, some transients could not be properly captured: e.g. during pump on-stroke (0.04 Δt_1 and 0.57 Δt_1) the simulated curve is somewhat steeper than the experimental trace indicates (Fig. 25).

During boom lowering the load acting on TBA is always overrunning and consequently pump delivery pressure should be lower than that required for boom lift. However, experimental and simulated pressures

shown in Fig. 24 and in Fig. 25 indicate that the pump APL enacts pressure control. This originates from the onset of a quite high back pressure as the bore chamber of TBA discharges flow through the OVC4 and the PDCV1 valves.

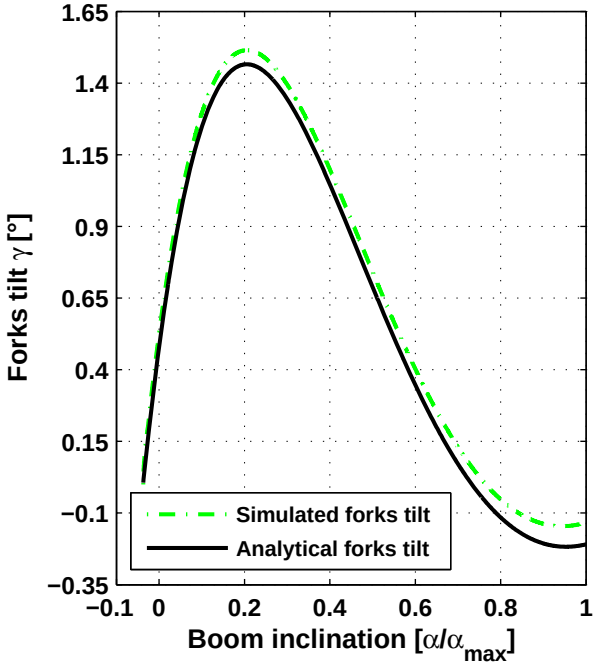

Fig. 23: *Analytical vs. Simulated forks tilt*

The pump works at partial displacement (82 % of maximum) with a correspondent linear speed of the boom actuator of about 0.16 m/s. In this situation, since the APL is in regulating conditions, retraction speed is load dependent. Furthermore, the difference between delivery and load sensing pressures is fairly constant at approximately 0,05 p_{max}. After about 0,85 Δt_1 seconds the rod of the TBA completes its inward travel with the associated onset of pressure oscillations (Fig. 24). Now a slow increase of P6 pressure signals (Fig. 25) can be observed during the boom lowering, again consequent to the boom force variation. Despite some cited limitations in the modelling phase, the predictive capability of system performance appears satisfactory.

Fig. 23 compares analytical vs. simulated fork tilt. A slight mismatch can be observed since in modelling the system, compressibility effects as well as leakages have been considered.

With reference to this work cycle Table 3 provides quantitative information about advantages of using the proposed Coupled Simulation approach.

Table 3: Solution times Coupled vs. Co-Simulation

Type	Communication Interval [ms]	CPU time [min]
Coupled	NA	29
Co-Simulation	1	179
Co-Simulation	2	93

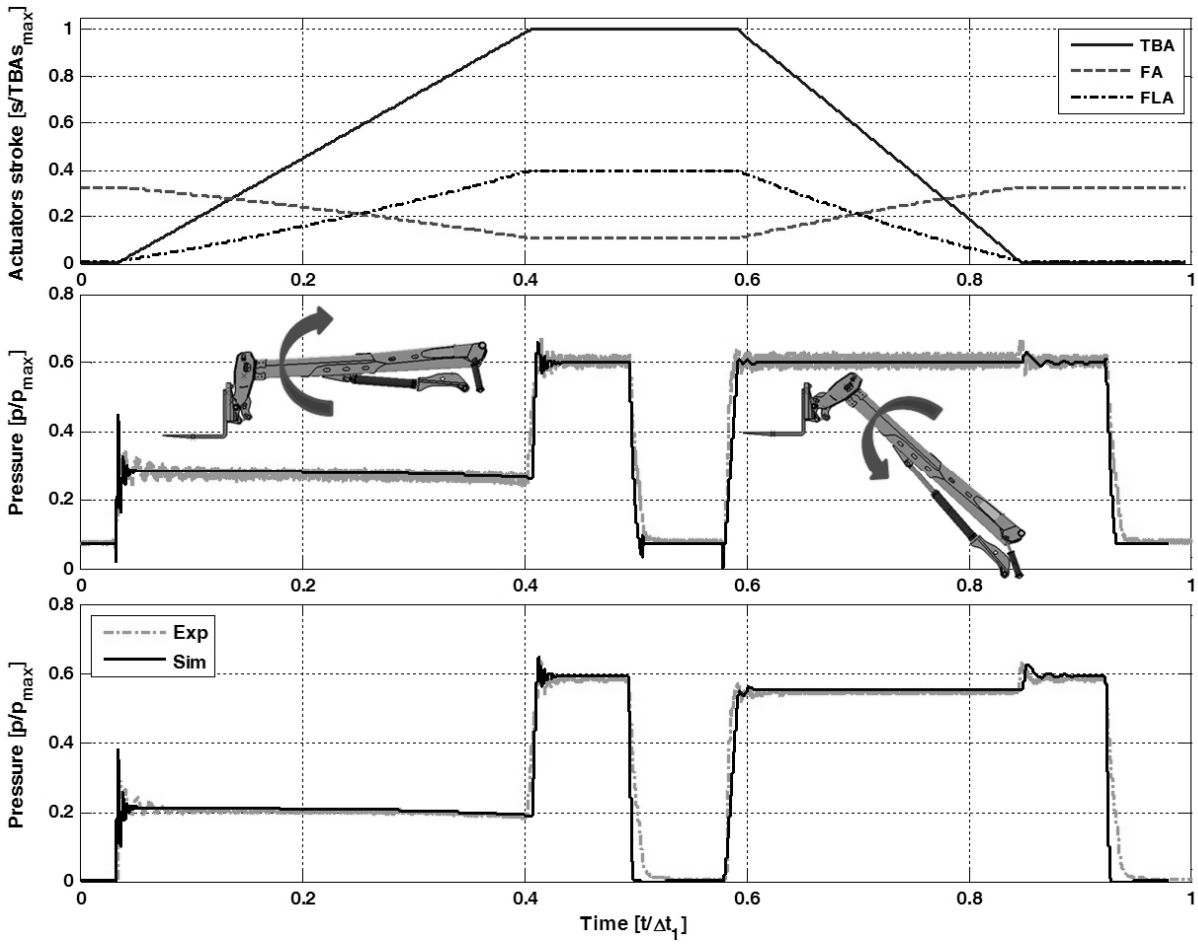

Fig. 24: *Actuators stroke(top) Pump delivery pressure P4 (middle); Load Sensing pressure P5 (bottom)*

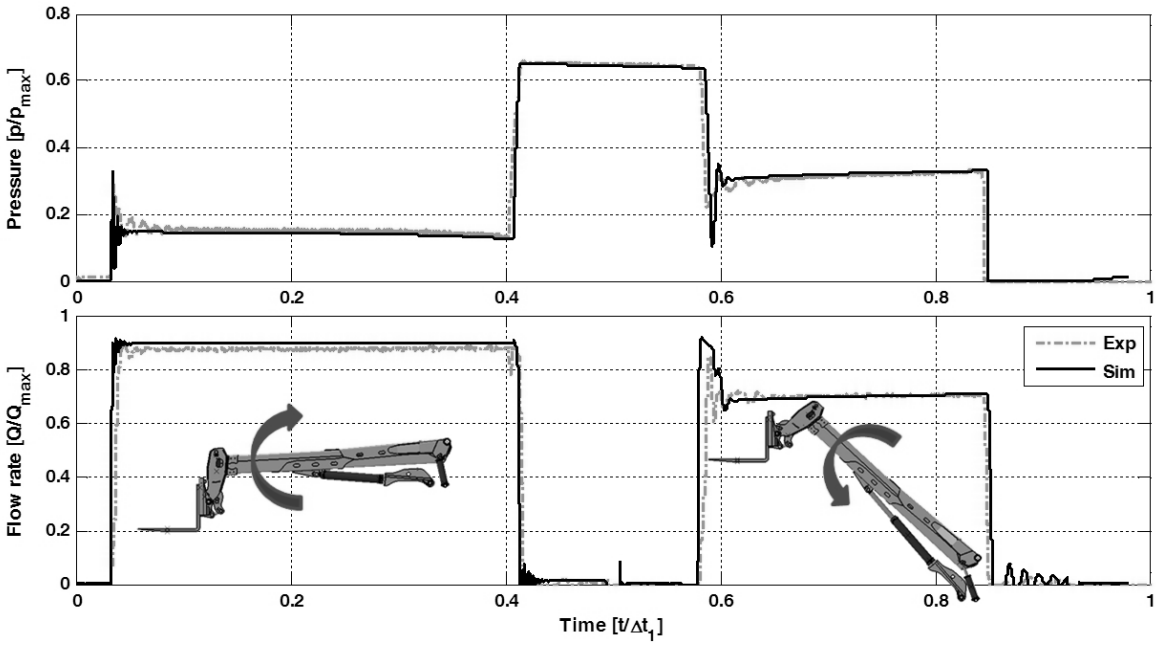

Fig. 25: *TBA bore side pressure P6 (top); Delivery flow rate Q (bottom)*

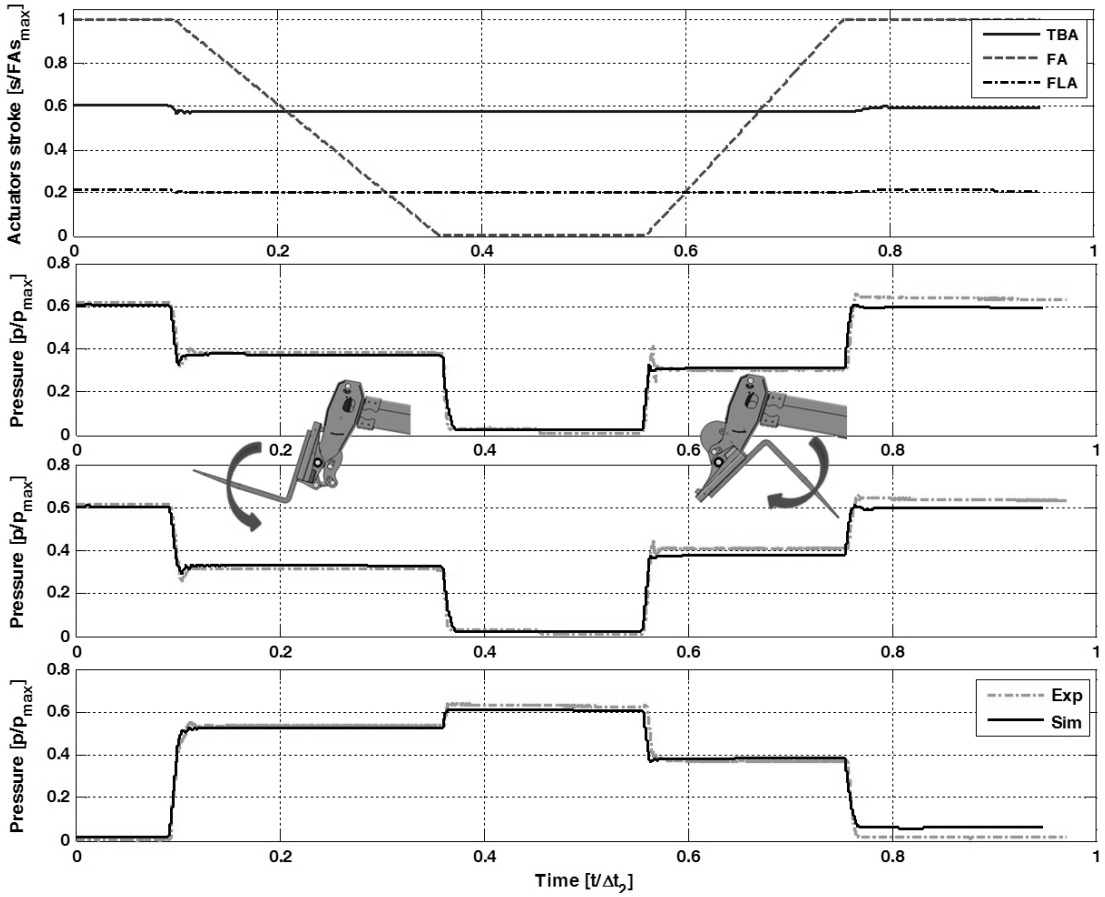

Fig. 26: *FA bore side pressure P1 (top); Dual OVC C2a port pressure P2 (middle); FA rod chamber pressure P3 (bottom)*

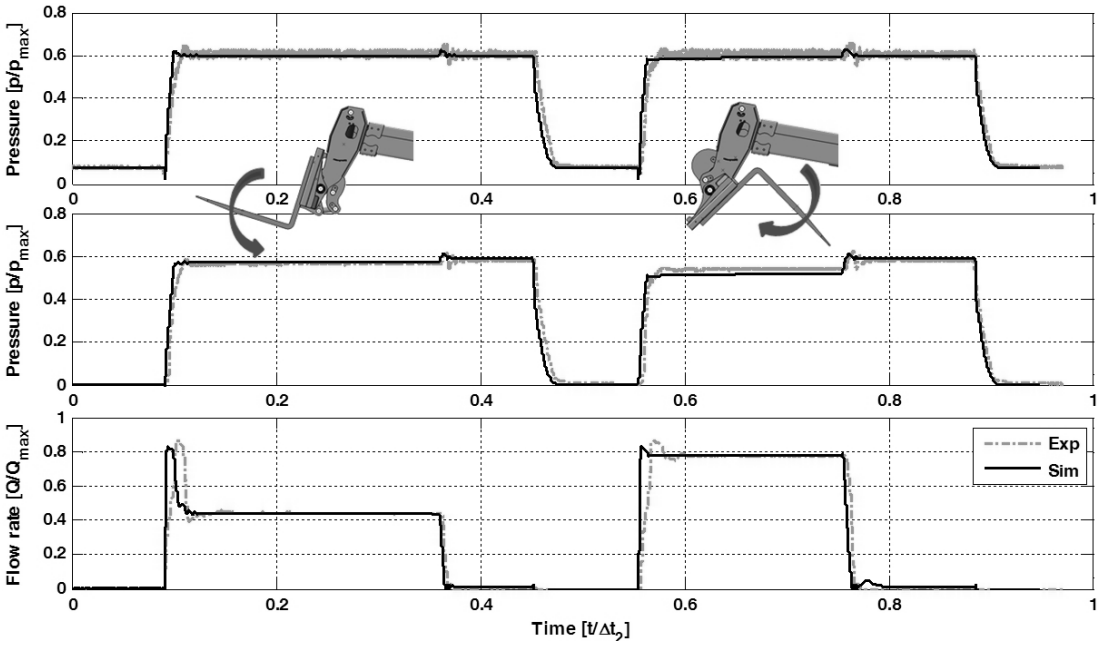

Fig. 27: *Delivery pressure P4 (top); Load Sensing pressure P5 (middle); and delivery flow rate Q (bottom)*

5.3 Forks Opening and Closing Cycle

This work cycle consists in the complete opening and closing of the forks leaving the boom directional valve at rest. The cycle is shown in Fig. 22 with a dashed line. After a short initial delay a command is issued through the joystick onto the PDCV2 aiming at opening the forks up to their maximum tilt. The pump delivery port is then connected with the rod chamber of the FA. The signal persists for a time period sufficient to complete forks opening via a complete retraction of the FA and thereafter guarantee the regulation of the APL. The command goes to zero and then is so enacted to feed pump flow rate to the bore chamber of the forks actuator. Also in this case, the signal persists for a time period sufficient to complete forks closing and grant pressure control through the pump APL (complete extension of the FA). In the initial idling condition pump delivery pressure is held at about 0.07 p_{max} by the DPL. Fig. 26 and Fig. 27 contrast experimental and simulated data pertinent to the forks work cycle. It is worth mentioning that, once the forks actuator in the outward stroke reaches its end stop, non-return valves NR3 and NR5 are responsible of the fact that pressurised fluid in the line connecting the bore chamber of FA and port C2a of the dual OVC valve becomes trapped. This clarifies why both at the start and end of the work cycle pressures P1 and P2 are not zero.

It can further be noticed that while forks are opened and closed pump delivery pressure is under control of the APL. Again flow rate through the directional control valve becomes load dependent. Experimental and simulated flow rates shown at the bottom of Fig. 27 are in very close match. As forks opening occurs the pump operates at partial displacement (53 % of maximum) delivering 0.44 Q_{max}. Pressures at other locations in the system are favourably close to experimental data: P1 and P3 are 3 % lower than experimental values instead P2 is 5 % higher. During forks closing the pump operates at 90 % of maximum displacement providing a flow rate of 0.78 Q_{max} that is in close match with experiments. One final remark regards observed oscillations of the boom (blue trace in the FA stroke in Fig. 26) when the forks actuator receives flow from the pump. This is consequent to the fact that when directing flow to the forks actuator chambers, the forks levelling actuator (FLA) becomes pressurized originating a disturbance thrust on the boom. This may represent an issue if boom positioning must comply with strict specifications.

6 Conclusions

The present work has highlighted interesting aspects related with a telehandler boom/forks kinematics and with its hydraulic system. Forks levelling error, forks lever ratio and force F_{TBA} were introduced and analysed. Experimental tests confirmed the theoretical trend of forces and lever ratios. Moreover, a detailed modelling of OVC valves combined with the multi-domain simulation model based on the coupling and interaction of the mechanical and hydraulic systems has permitted a thorough analysis of the boom and forks implemented on a commercial telehandler. The experimental validation has fairly established that the proposed modelling approach is adequate in its predictive capabilities if a system optimization is to be undertaken. This will minimize costs associated with the deployment of refurbished solutions and with field tests verifications.

Nomenclature

A_C	FLA surface of influence bore chamber	[mm^2]
a_c	FLA surface of influence rod side chamber	[mm^2]
A_F	FA surface of influence bore chamber	[mm^2]
a_f	FA surface of influence rod side chamber	[mm^2]
$A(x)$	Valve flow area	[mm^2]
C_q	Flow coefficient	[-]
FAs	Forks actuator stroke	[mm]
F_H	Reaction force in hinge H	[N]
F_{LOAD}	Load force acting on the forks	[N]
F_p	Force acting on the FA rod due to load	[N]
F_{TBA}	Force acting on the F_{TBA} rod due to load and boom weight	[N]
l_{cc}	Minimum distance between point M and A	[mm]
l_{fc}	Minimum distance between point C and E	[mm]
s	Generic actuator stroke	[mm]
TBAs	Telescopic boom actuator stroke	[mm]
x_p	Valve spool displacement	[mm]
α	Boom tilt	[°]
γ	Forks tilt with respect to γ_0	[°]
γ_0	Initial forks tilt (with stroke of TBA equal to zero)	[°]
δ	Jet angle of the fluid	[°]
$\Delta\pi$	Pressure drop	[bar]
Δt_1	Boom work cycle time window	[s]
Δt_2	Forks work cycle time window	[s]
θ	MBC angle	[°]
ζ	OBC angle	[°]

APL	Absolute pressure limiter
DPL	Differential pressure limiter
FA	Forks actuator
FLA	Forks levelling actuator
FLR	Forks lever ratio
TBA	Telescopic boom actuator
VLM	Virtual.Lab Motion

Acknowledgments

Authors wish to thank MERLO S.p.A. and LMS International.

References

Altare, G. 2009. *Analisi e Modellazione del Circuito Idraulico di un Miniescavatore*, MSc Thesis. Politecnico di Torino.

Prabhu, S. M. 2007. Model-Based Design for Off-Highway Machine Systems Development. *SAE Technical paper*, 2007-01-4248. doi: 10.4271/2007-01-4248.

Roccatello, A., **Mancò, S.** and **Nervegna, N.** 2007. Modelling a Variable Displacement Axial Piston Pump in a Multibody Simulation Environment, *J. Dyn. Sys., Meas., Control*, Vol. 29(4): pp. 456-469. doi: 10.1115/1.2745851.

Prescott, W. 2009. *Using multibody dynamics solvers in a multiphysics environment*. Multibody Dynamics, ECCOMAS Thematic Conference, Warsaw.

2010. *LMS Imagine.Lab AMESim Rev10: User manual*. LMS International.

2010. *LMS Virtual.Lab 9: User manual*. LMS International.

Hansen, R. H., **Andersen, T. O**. and **Pedersen, H. C.** 2010. *Development and implementation of an advanced power management algorithm for electronic load sensing on a telehandler*, Bath/ASME Symposium on Fluid Power and Motion Control 2010, Bath.

Gabriele Altare
Graduated in Mechanical Engineering (2009) from Politecnico di Torino. After graduation he joined the Fluid Power Research Laboratory of the Politecnico di Torino as a Ph.D. student. His research fields are mainly multibody simulation and hydraulic systems of earthmoving machines.

Francesco Lovuolo
Graduated in Mechanical Engineering (2009) from Politecnico di Torino. After graduation he joined the Fluid Power Research Laboratory of the Politecnico di Torino as a research fellow for 1 year. At present he works as consultant for Altran Italia S.p.A.

Nicola Nervegna
Graduate in Nuclear Engineering (1971) from Politecnico di Torino, Italy. He joined the Politecnico staff in October 1971 and, at present, is Professor of Fluid Power Systems.
His research interests lie in the broad fields of Fluid Power with involvement in positive displacement pumps as well as in the modelling, simulation and testing of various hydraulic components.

Massimo Rundo
Graduated in Mechanical Engineering (1996) from Politecnico di Torino. After graduation he participated within the Fluid Power Group of the Politecnico di Torino, as a Magneti Marelli visiting researcher, to an extensive and ongoing research project on gerotor and external gear pumps for internal combustion engines lubrication. He is very active in modelling, simulation and testing of fluid power components.